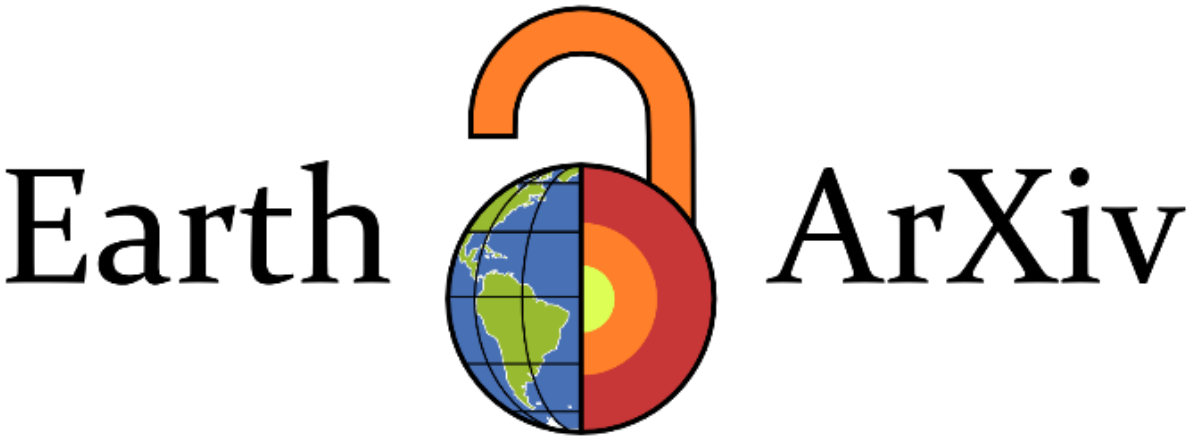


Peer review status:

This is a non-peer-reviewed preprint submitted to EarthArXiv.

Simulated heatwave increases CO_2 efflux from unvegetated saltpans and amplifies CH_4 efflux from vegetated saltmarshes

Sigit D Sasmito[1], Alexander Barkley[1], Lamberto Montagna[1], Brodie O'Breza[1], Most A. Linnas[2], Amrit K Mishra[1], Clement Duvert[3], Rory Mulloy[1], Paula Cartwright[1], Emily Douglas[4], Catherine E. Lovelock[5], Nathan J Waltham[2]

[1]Centre for Tropical Water and Aquatic Ecosystems Research (TropWATER), James Cook University, Townsville, QLD 4811, Australia

[2]College of Science and Engineering, James Cook University, Townsville, QLD 4811, Australia

[3]Research Institute for Environmental and Livelihoods (RIEL), Charles Darwin University, Casuarina, NT 0810, Australia

[4]Earth Sciences New Zealand, Hamilton, New Zealand, 3216

[5]School of the Environment, The University of Queensland, St Lucia QLD 4072

Corresponding author: sigitdeni.sasmito@jcu.edu.au

Abstract

Atmospheric heatwaves are increasing in frequency, intensity and duration under anthropogenic climate change, yet their effects on greenhouse gas (GHG) fluxes from coastal wetlands remain poorly understood. Coastal wetlands, including saltmarshes and saltpans (also called salt flat and sabkha), are globally significant carbon stores, but their vulnerability to extreme heat has rarely been tested experimentally. Here we report CO_2 and CH_4 fluxes over multiple days of simulated heatwaves using open-top chambers (OTCs) in three coastal wetland habitats in the dry tropics of Australia: unvegetated saltpan, and saltmarsh dominated by *Sarcocornia quinqueflora* or *Sporobolus virginicus*. We compared these with dry-season fluxes from the same site. OTCs warmed the surface by 3.3–4.5 °C in all habitats. Simulated heatwave shifted the saltpan from CO_2 uptake to emissions (p<0.05), whereas CO_2 efflux in both saltmarshes did not change significantly under OTCs. In *S. virginicus*, CO_2 efflux was insensitive to warming, indicating limited thermal effects on respiration. We identified vegetation cover, soil temperature and soil moisture as the main drivers of CO_2 efflux. CH_4 effluxes were low (<0.4 nmol m^{-2} s^{-1}) across sampled habitats, but increased three to five times from the dry to the wet season, and were further increased during simulated heatwaves in *S. quinqueflora*

(p<0.05). These contrasting responses suggest that vegetation shapes simulated heatwave effects on coastal wetland GHG fluxes through both physical and biological controls. Unvegetated saltpans may be particularly vulnerable to heatwave-driven CO_2 losses, while warming may increase CH_4 efflux from vegetated saltmarsh. Our results have implications for blue carbon conservation and managing coastal wetland carbon stocks in a warming world.

Keywords: blue carbon, coastal wetlands, greenhouse gas emissions, climate change mitigation, passive sediment warming

Introduction

Atmospheric heatwave events, characterised by periods of abnormally high temperatures over multiple days, have threatened ecosystems across climatic regions and are intensified under climate warming (Perkins-Kirkpatrick & Lewis, 2020; Xu et al., 2026). In tropical and subtropical Australia and other arid and semi-arid regions of the world, concurrent marine and atmospheric heatwaves already pose acute threats to coastal ecosystems, as evidenced by coral bleaching, macroalgae and seagrass loss events and as a contributing factor linked to the large-scale mangrove dieback across the north and western Australian coasts (Arias-Ortiz et al., 2018; Chung et al., 2023; Leggat et al., 2019; Smith et al., 2024). Marine heatwaves can contribute to the loss of biomass carbon stocks in seagrass and kelp ecosystems (Arias-Ortiz et al., 2018; Filbee-Dexter et al., 2026). It has been well established and well evidenced that atmospheric heatwaves have negative impacts on terrestrial ecosystem productivity and soil greenhouse gas (GHG) emissions (An et al., 2022; Bastos et al., 2014; Ciais et al., 2005). However, little is understood about how heatwaves affect changes in carbon greenhouse fluxes in coastal wetlands.

Coastal wetlands, often known as blue carbon ecosystems, include mangroves, saltmarshes, seagrass, salt- and tidal-flats, tidal forested wetlands and macroalgae (Adame et al., 2024; Lovelock & Duarte, 2019) are widely recognised as important natural carbon sinks (Macreadie et al., 2021; Rosentreter et al., 2023). Their anaerobic, waterlogged sediments accumulate organic carbon at rates exceeding carbon dioxide (CO_2) and methane (CH_4) released to the atmosphere through organic matter decomposition and metabolism (Malerba et al., 2022; Poffenbarger et al., 2011; Rosentreter et al., 2021). Although CO_2 and CH_4 fluxes from coastal wetland sediments are strongly governed by environmental and climatic drivers such as temperature, tidal inundation and salinity (Al-Haj & Fulweiler, 2020; Iram et al., 2021; Rosentreter et al., 2023), vascular plants can modify how these fluxes respond to warming through different mechanisms. Plant canopies shade the sediment

surface, buffering sediment temperature and potentially reducing the thermal response of microbial respiration (Whitcraft & Levin, 2007). Extended periods of warming may contribute to an increase in transpiration and radial oxygen loss from roots, suppressing methanogenesis and stimulating methanotrophy (Määttä & Malhotra, 2024). Heat stress may also increase inputs of labile carbon from root exudates and damaged tissues, fuelling CO_2 production and, where sulphate is limited, promoting methanogenesis (Lei et al., 2023). In contrast, unvegetated sediments are directly exposed to solar heating and evaporation, which may amplify microbial responses or, where hypersalinity develops, inhibit them. Consequently, vegetated and unvegetated habitats within the same landscape may differ in their thermal sensitivity of GHG emissions.

Saltmarshes in Australia account for 4% of the world's saltmarsh area (Worthington et al., 2024), while saltpans habitat extent has rarely been characterised (Hickey et al., 2025). These habitats are often adjoining within high intertidal landscapes and are distributed extensively across northern Australia, including the Gulf of Carpentaria, Exmouth Gulf and Pilbara regions in Western Australia and Central to South Queensland (DETSI, 2019; Hickey et al., 2025). Saltmarsh habitats in Central Queensland are dominated by communities called samphires comprised of succulent plants in the genera *Tecticornia*, *Sarcocornia* and *Suaeda*, as well as communities dominated by the C_4 grass *Sporobolus virginicus* (Queensland Government, 2019). While *S. virginicus* can grow in dense forms that cover the sediment surface, plants in samphire are often sparsely distributed. These contrasting canopy cover and structure conditions may differentially affect carbon cycling mechanisms. Saltpans lack emergent vegetation because of hypersalinity, but support cyanobacterial mats (Hickey et al., 2025). These mats lie dormant when dry and rapidly reactivate photosynthesis and grow during inundation with tidal water or during rainfall (Adame et al., 2012; Lovelock et al., 2010), potentially supplying labile carbon to sediment microbes. Understanding how coastal wetland ecosystems and their ecological functioning respond to short-duration, but intense, air temperature anomalies is therefore a pressing scientific and management priority, particularly in the context of heatwave effects on the permanence of climate mitigation services offered by coastal wetlands conservation and restoration.

In this study, we focus on assessing carbon cycling in high-intertidal saltmarshes and saltpans of dry tropical northern Australia. We aimed to characterise the impacts of heatwave events on their ecosystem (plants and sediments) CO_2 and CH_4 effluxes. We experimentally applied multiple days of simulated heatwave in replicate field plots using open-top chambers (OTC), which provided a passive sediment warming intervention (Douglas et al., 2025). Across two saltmarsh habitats (dominated by *Sarcocornia quinqueflora* and *Sporobolus virginicus)* and in unvegetated saltpans we measured the CO_2 and CH_4 fluxes in heated plots during low tide in the summer wet season and compared these to

control plots, and previous measurements during the dry winter period. We expected GHG emissions in unvegetated saltpan habitats to be lower than at other vegetated saltmarshes. Simulated heatwaves were expected to increase emissions more in vegetated habitats than in saltpans, where greater labile-carbon availability could support CO_2 and CH_4 emissions. (Lewis et al., 2026). Additionally, we anticipated that summer wet season emissions would be higher than during the dry winter period (Adame et al., 2026). Our results provide the first experimental evidence of habitat-specific heatwave responses in greenhouse gas (GHG) fluxes from Australian saltmarshes, which contributes to the understanding of the temperature sensitivity of coastal wetlands carbon cycling (Carey et al., 2022; Douglas et al., 2025; Sang et al., 2026). This study has important benefits for the management and conservation of carbon permanence in blue carbon ecosystems under accelerating climate change.

Methods

Study site

The study was conducted at Oonoonba Wetlands (approximately 19.3°S, 146.7°E, Figure 1), a coastal wetland complex located in Townsville, north Queensland, Australia (Sasmito et al., 2026). The site was representative of high intertidal ecosystems within the dry tropics, characterised by a strong contrast in seasonal climate conditions, with a wet season from November to April and a pronounced cooler dry season (May to October) (Table S1). The wetland contains a mosaic of habitat types along the intertidal elevation gradient, including unvegetated saltpan, saltmarsh communities dominated by *S. quinqueflora and S. virginicus*, with mangroves occurring along the main tidal creek connected to Ross River. All measurements and heatwave simulations were conducted during the summer-wet season.

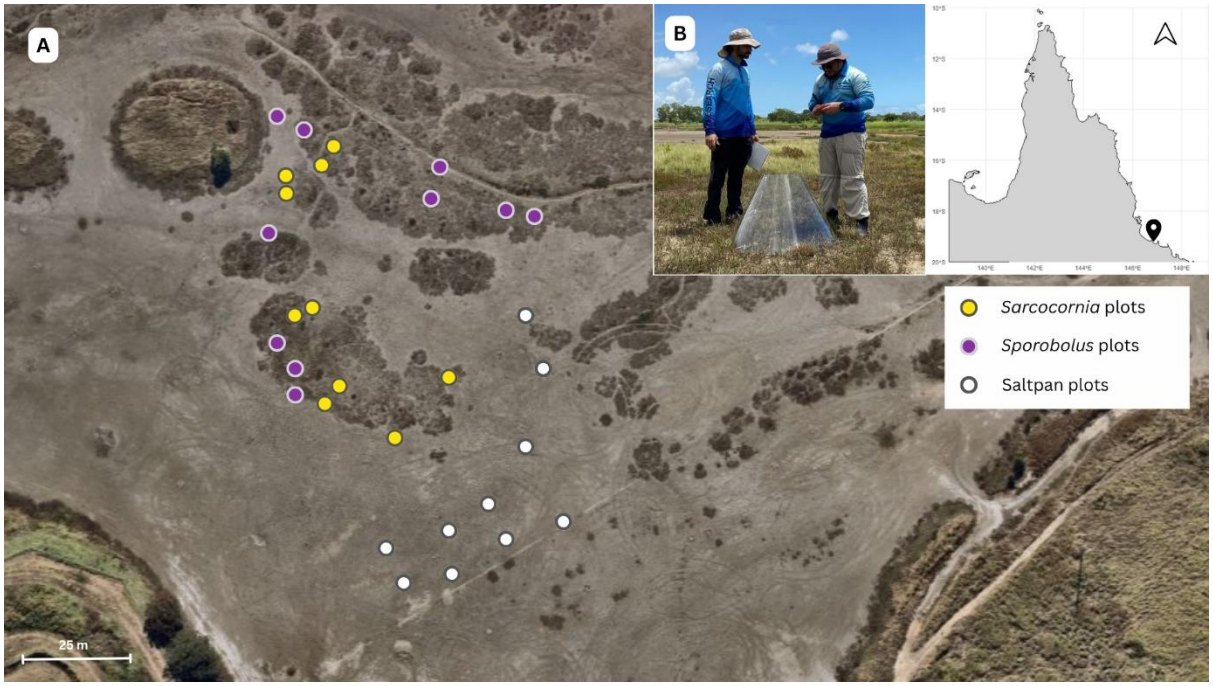


Figure 1. Map of study site and sampling plots distribution across saltpans, *Sarcocornia quinqueflora and Sporobolus . virginicus* in Oonoonba wetlands, north Queensland.

Experimental design

Simulated heatwave plots were established using open-top warming chambers (OTC) constructed from clear 1.5mm thick polycarbonate sheeting, designed to passively elevate air and surface soil temperatures within the enclosed plot (Douglas et al., 2025). The OTC design and dimensions (0.8 m base diameter, 0.3 top diameter and 0.5 m height) followed the previous study in intertidal estuarine sediments (Douglas et al., 2025). Paired OTC (n=5) and control (non-OTC, n=5) plots were established within each of the three habitat types: saltpan, *S. quinqueflora* (succulent saltmarsh), and *S. virginicus* (herbaceous saltmarsh)—OTCs were 6 plots here (Table 1). OTCs were installed in fixed positions between 09:30–13:30 each day and 11:00–15:00 on 11 March, and CO_2 and CH_4 fluxes were measured directly after OTC removal. The heatwave simulation was maintained for seven consecutive days (10–16 March 2026), with gas flux measurements conducted daily throughout the experimental period (Figure 2). For control plots, measurements were conducted mostly in the morning on all days (Days 1–7). For OTC (simulated heatwave) plots, measurements commenced on Day 2 and followed on Days 4, 5 and 7. Rainfall occurred occasionally over the study period, especially during midday and afternoon on Days 3 and 7 (See Table 1), which resulted in less significant changes in sediment temperature between inside and outside OTC plots (Table 1).

Table 1. Site, sampling design, vegetation, soil properties, environmental conditions, weather and tides in three coastal wetland types at Oonoonba Wetlands (Townsville, north Queensland) in the dry season (August 2025) and during the simulated heatwave in the wet season (March 2026; Control and open-top chamber (OTC), plots).

	Saltpan			Saltmarsh *Sarcocornia*			Saltmarsh *Sporobolus*		
Variable	**Dry 2025**	**Wet 2026 Control**	**Wet 2026 OTC**	**Dry 2025**	**Wet 2026 Control**	**Wet 2026 OTC**	**Dry 2025**	**Wet 2026 Control**	**Wet 2026 OTC**
Sampling design									
Sampling dates	7, 19 Aug 2025	10–14, 16 Mar 2026	11, 13, 14, 16 Mar 2026	7, 19 Aug 2025	10–14, 16 Mar 2026	11, 13, 14, 16 Mar 2026	7, 19 Aug 2025	10–14, 16 Mar 2026	11, 13, 14, 16 Mar 2026
Measurement days	–	1, 2, 3, 4, 5, 7	2, 4, 5, 7	–	1, 2, 3, 4, 5, 7	2, 4, 5, 7	–	1, 2, 3, 4, 5, 7	2, 4, 5, 7
Plots (n)	5	5	5	5	5	5	5	5	6
CO_2 flux measurements (n)	10	21	18	11	22	18	15	19	21
CH_4 flux measurements (n)	8	16	15	10	19	17	13	10	19
Vegetation and fauna									
Vegetation cover (%)	–	0 ± 0 (4)	0 ± 0 (5)	–	36 ± 9 (5)	49 ± 12 (5)	–	92 ± 1 (4)	82 ± 5 (6)
Crab burrows (n per collar)	–	0.0 ± 0.0 (4)	0.0 ± 0.0 (5)	–	4.0 ± 1.6 (5)	5.6 ± 1.1 (5)	–	11.0 ± 3.7 (4)	8.3 ± 2.9 (6)
Soil properties									
Soil organic matter (%)	–	3.89 ± 0.21 (3)	4.16 ± 0.16 (5)	–	5.22 ± 0.46 (5)	7.83 ± 0.78 (5)	–	6.67 ± 1.91 (4)	4.24 ± 0.47 (5)
Carbon content (%)	–	1.35 ± 0.08 (3)	1.46 ± 0.06 (5)	–	1.88 ± 0.19 (5)	2.92 ± 0.31 (5)	–	2.46 ± 0.76 (4)	1.48 ± 0.19 (5)
Bulk density (g cm^{-3})	–	0.69 ± 0.07 (3)	1.22 ± 0.07 (5)	–	0.84 ± 0.06 (5)	1.25 ± 0.06 (5)	–	1.06 ± 0.09 (4)	1.03 ± 0.07 (5)
Soil WFPS (%)	22.6 ± 3.2 (4)	34.6 ± 1.5 (3)	39.5 ± 0.3 (5)	19.2 ± 1.2 (4)	36.0 ± 2.3 (5)	39.7 ± 1.6 (5)	34.7 ± 2.4 (5)	41.4 ± 4.0 (4)	45.4 ± 1.7 (5)
Temperature monitoring									
Air temperature inside chamber during flux measurement (°C)	28.0 ± 0.6 (16)	36.9 ± 0.6 (21)	37.7 ± 0.6 (18)	28.1 ± 0.8 (11)	35.8 ± 0.4 (22)	34.6 ± 0.5 (18)	27.0 ± 0.6 (15)	34.1 ± 0.6 (19)	32.5 ± 0.3 (21)
Soil temperature at 1 cm after OTC is removed or during flux measurement inside OTC (°C)	–	–	34.5 ± 0.5 (18)	–	–	33.2 ± 0.5 (18)	–	–	31.3 ± 0.4 (21)
Soil temperature 1 cm, outside OTC or control (°C)	–	–	33.1 ± 0.5 (14)	–	–	32.6 ± 0.5 (18)	–	–	31.5 ± 0.3 (20)
OTC warming during heatwave window, ΔT (°C)	–	–	+4.1 ± 2.2 (7)	–	–	+3.3 ± 2.5 (4)	–	–	+4.5 ± 3.7 (5)
Weather and tides on sampling days									
Daily rainfall on sampling days (mm), mean (range)	0.0 (0.0–0.0)	5.6 (0.0–14.8)	5.2 (0.0–14.8)	0.0 (0.0–0.0)	5.6 (0.0–14.8)	5.2 (0.0–14.8)	0.0 (0.0–0.0)	5.6 (0.0–14.8)	5.2 (0.0–14.8)
Rainfall in the 30 days before sampling (mm)	16.4	393.6	393.6	16.4	393.6	393.6	16.4	393.6	393.6
Daily maximum air temperature (°C), mean (range)	27.8 (27.2–28.4)	31.0 (30.1–31.7)	31.0 (30.1–31.7)	27.8 (27.2–28.4)	31.0 (30.1–31.7)	31.0 (30.1–31.7)	27.8 (27.2–28.4)	31.0 (30.1–31.7)	31.0 (30.1–31.7)
Highest daily high tide (m), range	3.40–3.57	2.59–3.56	2.79–3.56	3.40–3.57	2.59–3.56	2.79–3.56	3.40–3.57	2.59–3.56	2.79–3.56
Lowest daily low tide (m), range	0.61–0.66	0.94–1.85	0.94–1.66	0.61–0.66	0.94–1.85	0.94–1.66	0.61–0.66	0.94–1.85	0.94–1.66

	Saltpan			Saltmarsh *Sarcocornia*			Saltmarsh *Sporobolus*		
Variable	**Dry 2025**	**Wet 2026 Control**	**Wet 2026 OTC**	**Dry 2025**	**Wet 2026 Control**	**Wet 2026 OTC**	**Dry 2025**	**Wet 2026 Control**	**Wet 2026 OTC**
Time of daytime low tide	12:50–13:39	12:47–14:17	12:47–14:17	12:50–13:39	12:47–14:17	12:47–14:17	12:50–13:39	12:47–14:17	12:47–14:17

a. Values are mean ± SE (n). Plot-level variables (vegetation cover, crab burrows, soil properties, WFPS) are averaged per plot; environmental variables and fluxes per flux measurement (dark chambers). OTC warming is mean ± SD (n simulated heatwave windows).

b. Vegetation cover refers to vascular plants; salt-flat plots were covered by microbial mats (recorded as 0 %). Vegetation cover, crab burrows and soil properties were not recorded in 2025.

c. Chamber air temperature was recorded inside the flux chamber during each measurement. OTCs were removed before flux measurements, so air temperature reflects ambient conditions at the time of measurement.

d. Soil temperature at 1 cm was recorded at OTC plots only, inside and immediately outside the OTC position, at the time of flux measurement. OTC warming (ΔT) is the mean difference between OTC and paired control loggers during each daily heatwave window (09:30–13:30; 11:00–15:00 on 11 March), one logger pair per wetland type (two OTC loggers on the saltpan).

e. – = not measured.

f. Weather from Bureau of Meteorology station 032040 (Townsville Aero, 19.25°S, 146.77°E). Daily rainfall is the 24 h total to 09:00 on the date given. Rainfall in the 30 days before sampling is counted back from the first sampling day (7 Aug 2025; 10 Mar 2026, heatwave Day 1). Values are site-level and repeated for each wetland type.

g. Tides are Bureau of Meteorology predictions for Townsville (heights above Lowest Astronomical Tide). Daytime low tides fell within or just after the 09:30–13:30 measurement window on all sampling days. The heatwave week moved from neap tides (last quarter moon, 11 Mar 2026) towards spring tides; August 2025 sampling was two days before full moon (7 Aug) and four days before new moon (19 Aug).

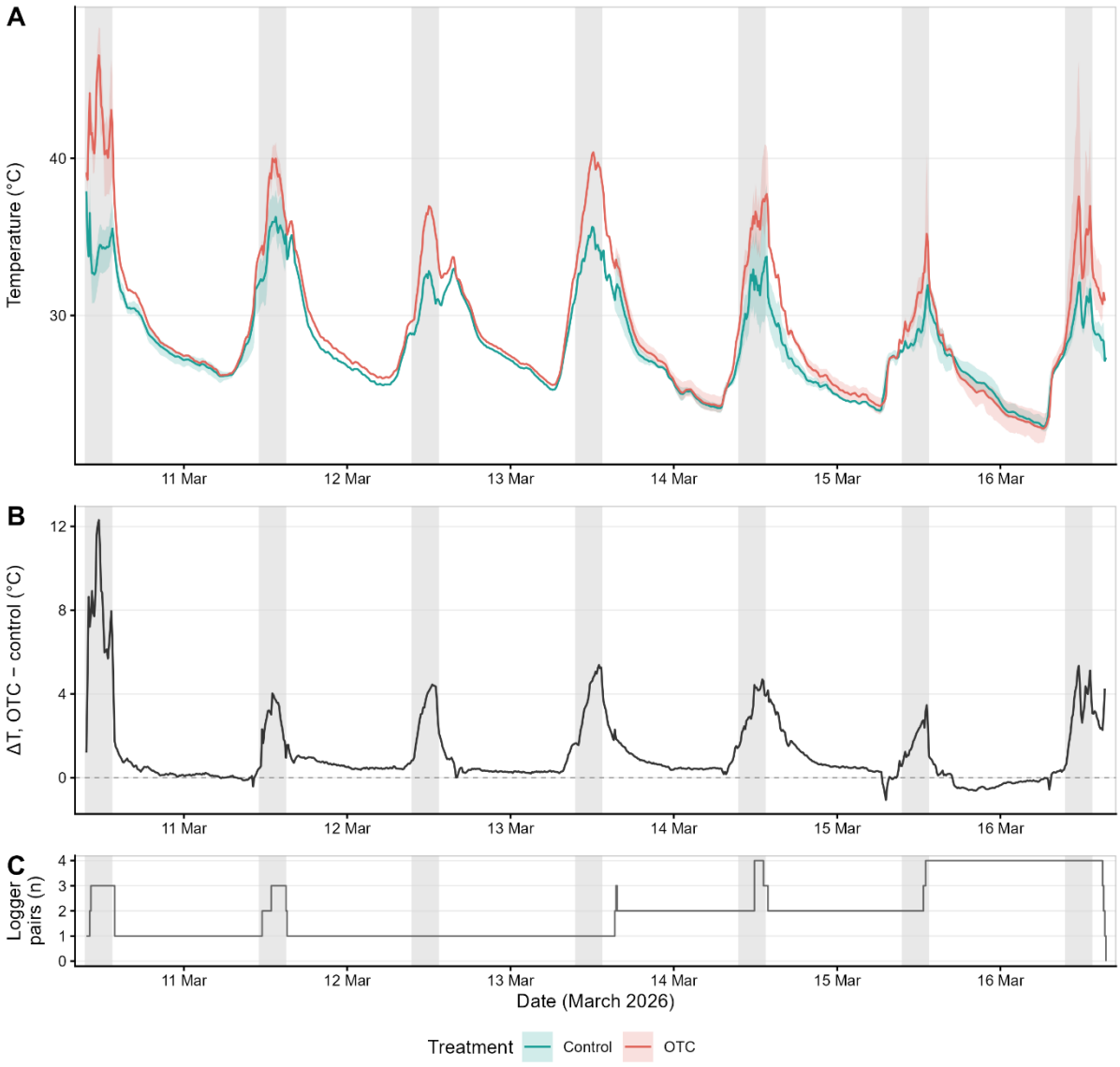


Figure 2. Temperature during the simulated heatwave combined across wetland types. (A) Mean temperature of OTC and control loggers (lines), with the range across loggers (bands). **(B)** Mean warming (OTC minus paired control). **(C)** Number of logger pairs recording at each time. From 11 to 13 March, only the salt-flat pair was recording due to limited availability of the temperature loggers. Grey bands mark daily simulated heatwave windows.

CO_2 and CH_4 fluxes measurements

Carbon dioxide and methane fluxes were measured using a closed dynamic chamber approach that incorporated all above- and below-ground living biomass, including saltmarsh vegetation and the cyanobacterial mat on saltpans. The inclusion of plant biomass in the flux measurement means that the flux value represents flux from both vegetation and sediments. A portable gas analyser (LICOR

7810) was connected to dark acrylic dome hemisphere chambers (15.24cm diameter and 7.62cm height) attached with 5cm collars (Figure 1). Concentrations of CO_2 (µmol mol^{-1}) and CH_4 (nmol mol^{-1}) were logged continuously for 5 minutes with the chamber closed. Fluxes were calculated from the linear rate of concentration change within the chamber incubation period, corrected for chamber volume, collar area, air temperature, and atmospheric pressure according to standard methods (Equation 1). Measurements were conducted at approximately the same time of day across all sampling occasions to minimise confounding effects from possible diurnal variation in flux rates. CO_2 efflux is reported in units of µmol CO_2 m^{-2} s^{-1} and CH_4 efflux in units of nmol CH_4 m^{-2} s^{-1}, with positive values indicating net emission to the atmosphere and negative values indicating net uptake.

$$F = \frac{dsc}{dt} \cdot \frac{P \cdot V}{R \cdot T_{air} \cdot A} \qquad \text{(Equation 1)}$$

Where: F: Gas efflux (µmol CO_2 m^{-2} s^{-1} or nmol CH_4 m^{-2} s^{-1}), P : Air pressure (Pa), V : Total chamber headspace volume (m^3), including collar volume, A : Soil surface area enclosed by the collar (m^2), R : Universal gas constant (8.314 Pa m^3 K^{-1} mol^{-1}), Tair : Air temperature (K), dsc/dt : rate of change of dry mole fraction of CO_2 or CH_4 (µmol CO_2 mol dry air^{-1} s^{-1} or nmol CH_4 mol dry air^{-1} s^{-1}).

Environmental parameters

Air and sediment surface temperature were recorded continuously at 1-min intervals with portable temperature loggers (EnvLoggers, Hardware T2.4). These were placed inside one OTC and one adjacent control plot in each wetland type, with a second OTC logger deployed on the saltpan, at 1-cm below the sediment surface from 10 to 16 March 2026. At each flux measurement, chamber air temperature was recorded inside the flux chamber, and soil temperature at 1 cm depth was measured inside and outside the OTC (EnvLoggers, Hardware T2.4). Sediment cores (diameter 5cm and 5cm thickness) were collected once from each plot on Day 7 to determine bulk density (dry mass per unit volume after oven-drying at 60°C for three days or until constant weight), and soil organic matter using the Loss on Ignition method. For Loss on Ignition, soil was combusted at 550 °C for four hours. Sediment water-filled pore space (WFPS) was calculated from gravimetric water content and bulk density, assuming a particle density of 2.65 g cm^{-3} (Iram et al., 2021; Sasmito et al., 2026). Vegetation cover (%) and the number of crab burrows were recorded visually within the area enclosed by each collar. Daily rainfall and maximum air temperature were obtained from the Bureau of Meteorology station at Townsville Aero (station 032040; 19.25°S, 146.77°E). Tide heights for Townsville were taken from Bureau of Meteorology tide predictions, referenced to Lowest Astronomical Tide.

Statistical analysis

Differences in CO_2 and CH_4 flux among the dry season (August 2025), the wet season control and the wet season OTC plots (March 2026) were assessed separately for each wetland type as the heatwave simulation was only performed during the wet season. We used Kruskal–Wallis tests followed by Dunn's pairwise comparisons with Holm-adjusted p-values, because flux data were not normally distributed despite data transformation (Shapiro–Wilk test). CH_4 fluxes were displayed on an inverse hyperbolic sine (asinh) scale to accommodate negative values and a skewed distribution. Daily flux dynamics during the heatwave are shown in Figure S2. OTC warming was quantified from the continuous loggers as the mean temperature difference between each OTC and its paired control logger during each daily heatwave window (09:30–13:30; 11:00–15:00 on 11 March). Windows with less than 50% logger coverage were excluded.

To identify drivers of CO_2 and CH_4 efflux, we fitted random forest models (ranger package; 1,000 trees, minimum node size 3) for each gas, with CH_4 asinh-transformed. Predictors were vegetation cover, crab burrows, soil organic matter, bulk density, WFPS, soil temperature at 1 cm, chamber air temperature, wetland type and treatment. Predictors were included only if they were available for both treatments, and where correlations among predictor variables did not exceed a Spearman correlation of $\rho = 0.71$. To assess whether results were affected by the contrast between the saltpan and the saltmarsh, models were refitted using saltmarsh plots only. Relationships between gas fluxes and individual environmental variables were assessed with Spearman rank correlations, with temperature relationships tested separately for each wetland type. All analyses were conducted in R (version 4.6.1; R Core Team 2026) using dplyr, tidyr, rstatix, multcompView, ranger, kernelshap, shapviz, ggplot2 and ggpubr.

Results

Simulated heatwave elevated sediment CO_2 efflux in the saltpan but not in vegetated saltmarsh

During the simulated heatwave, the OTCs warmed the surface sediment by an average of 3.3–4.5 °C relative to paired controls during daily deployment windows (Figure 2, S2). Soil temperature at 1 cm at the time of flux measurement was highest in the saltpan and lowest under the dense *S. virginicus* canopy (34.5 ± 0.5, 33.2 ± 0.5 and 31.3 ± 0.4 °C in saltpan, *S. quinqueflora* and *S. virginicus* OTC plots, respectively; Figure 3C; Table 1). In the saltpan, CO_2 efflux was significantly higher in OTC than control plots (0.25 ± 0.15 vs −0.35 ± 0.09 μmol m^{-2} s^{-1}; $p < 0.05$; Figure 3A). Control plots showed net CO_2 uptake on all measurement days, whereas median efflux in OTC plots was positive on all days except

Day 7, which followed 14.8 mm of rainfall (Table 1). In contrast, CO_2 efflux in the *S. quinqueflora* and *S. virginicus* saltmarshes did not differ significantly between OTC and control plots (Figure 3A). In *S. quinqueflora*, however, median efflux was higher in OTC plots on every measurement day (Figure S3). CO_2 efflux was consistently higher in the vegetated saltmarshes than in the saltpan, and highest in *S. virginicus* (2.98 ± 0.33 and 3.07 ± 0.24 μmol m^{-2} s^{-1} in control and OTC plots), which also showed the greatest day-to-day variability (Figure 3A; Figure S4). In both saltmarshes, wet season CO_2 efflux was two to three times higher than in the 2025 dry season (*S. quinqueflora*: 0.70 ± 0.05; *S. virginicus*: 1.22 ± 0.11 μmol m^{-2} s^{-1}). This difference in CO_2 efflux between dry and wet seasons was significant for *S. virginicus* and also between the dry season and the OTC plots during the wet season for *S. quinqueflora* (Figure 3A).

Warming amplified a strong seasonal increase in CH_4 efflux

CH_4 efflux was low across all habitats (<0.4 nmol m^{-2} s^{-1} on average) but was three to five times higher in the wet season than in the dry season in all three habitats ($p < 0.05$; Figure 3B). Within the wet season, CH_4 efflux was higher in OTC than in control plots in all habitats. The difference was significant only in *S. quinqueflora*, where efflux increased from 0.231 ± 0.064 to 0.385 ± 0.086 nmol m^{-2} s^{-1} ($p < 0.05$; Figure 3B). In *S. virginicus*, mean efflux in OTC plots was nearly four times that of controls (0.331 vs 0.088 nmol m^{-2} s^{-1}), but this difference was not significant, reflecting high variability among plots (Figure 3B).

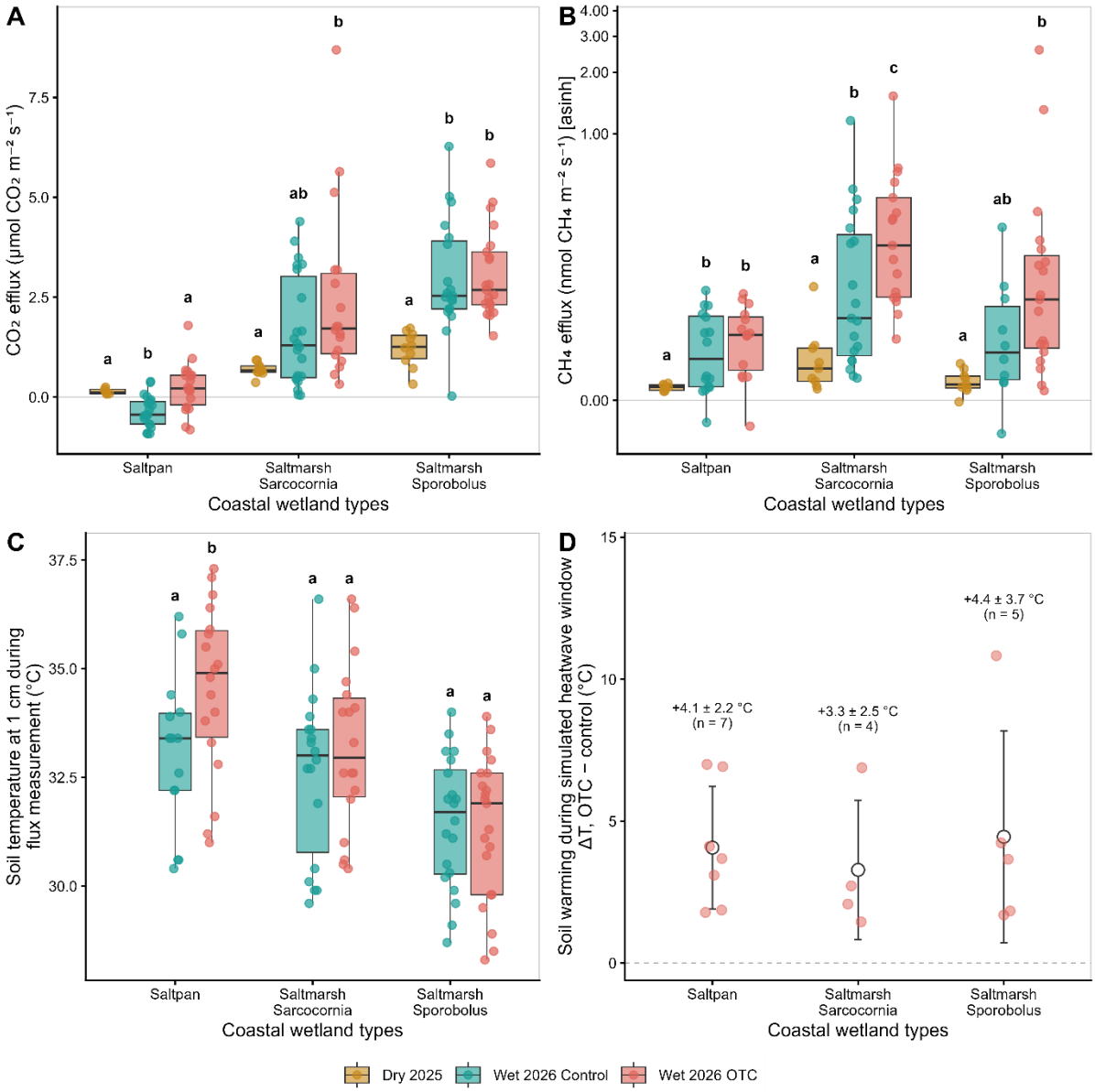


Figure 3. Soil CO_2 and CH_4 fluxes, and temperature in three coastal wetland types at Oonoonba Wetlands in the dry season (August 2025) and during a simulated heatwave in the wet season (March 2026). (A) CO_2 and **(B)** CH_4 efflux in the dry season and in control and open-top chamber (OTC) plots during the simulated heatwave; CH_4 is shown on an inverse hyperbolic sine (asinh) scale. **(C)** Soil temperature at 1 cm depth at the time of flux measurement in control and OTC plots. **(D)** OTC warming during the heatwave, calculated as the mean soil temperature difference between OTC and paired control loggers during each daily deployment window (09:30–13:30; 11:00–15:00 on 11 March). In A–C, each box shows the interquartile range (25th–75th percentiles) and the horizontal line is the median. Whiskers reach the most extreme values within 1.5 × IQR of the box edges. Letters compare groups within each wetland type. In D, Open circles show the mean across simulated

heatwave windows and error bars show ± 1 SD. Values above the bars are mean ± SD, with n = number of heatwave windows.

Vegetation cover and soil temperature were the main drivers of CO_2 efflux

The random forest model explained a substantial part of the variation in CO_2 efflux (R^2 = 0.59; Figure 4A). Vegetation cover was by far the most important predictor, with higher cover associated with greater CO_2 efflux (Figure 4A-B), followed by wetland type, soil temperature at 1 cm and WFPS. Warmer soils and wetter sediments were associated with higher CO_2 efflux (Figure 4B, 5). The warming effect on CO_2 efflux was captured by measured soil temperature (Figure 2). Vegetation cover remained the dominant predictor, and soil temperature the second, when the saltpan was excluded (Figure S5), so their effects were not simply a contrast between vegetated and unvegetated habitats. In contrast, the measured variables explained very little of the variation in CH_4 efflux (R^2 = 0.03), and the ranking of predictors was unstable among models (Figure 4D–F; Figure 5).

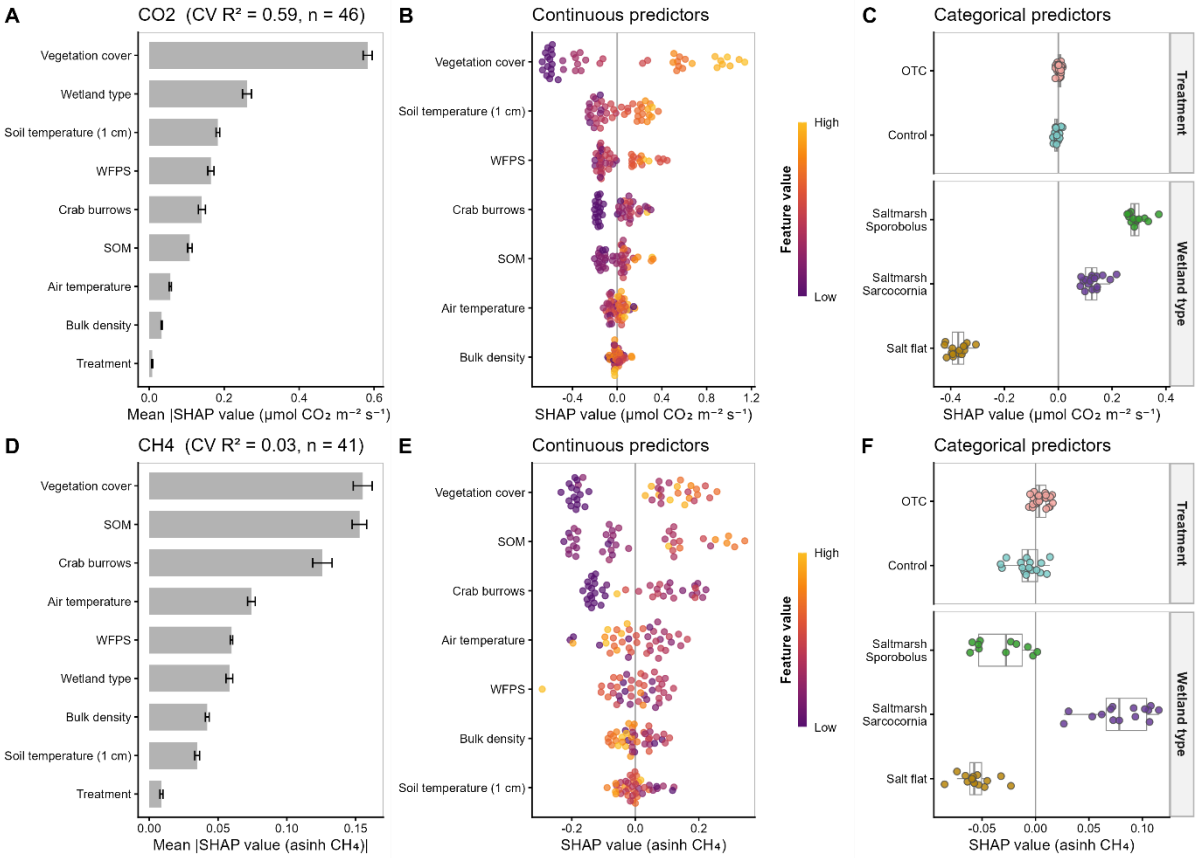


Figure 4. Drivers of soil CO_2 (A–C) and CH_4 (D–F) effluxes during the simulated heatwave, identified with random forest models and SHAP (SHapley Additive exPlanations) values. (A, D) Predictor

importance as mean absolute SHAP value for CO_2 and CH_4 respectively; bars show the mean and error bars the SD across 10 model fits with different random seeds. **(B, E)** SHAP values for continuous predictors; each point is one flux measurement, coloured from low (purple) to high (yellow) predictor value. Positive SHAP values indicate that the predictor increased the predicted flux. (C, F) SHAP values for categorical predictors (treatment and wetland type).

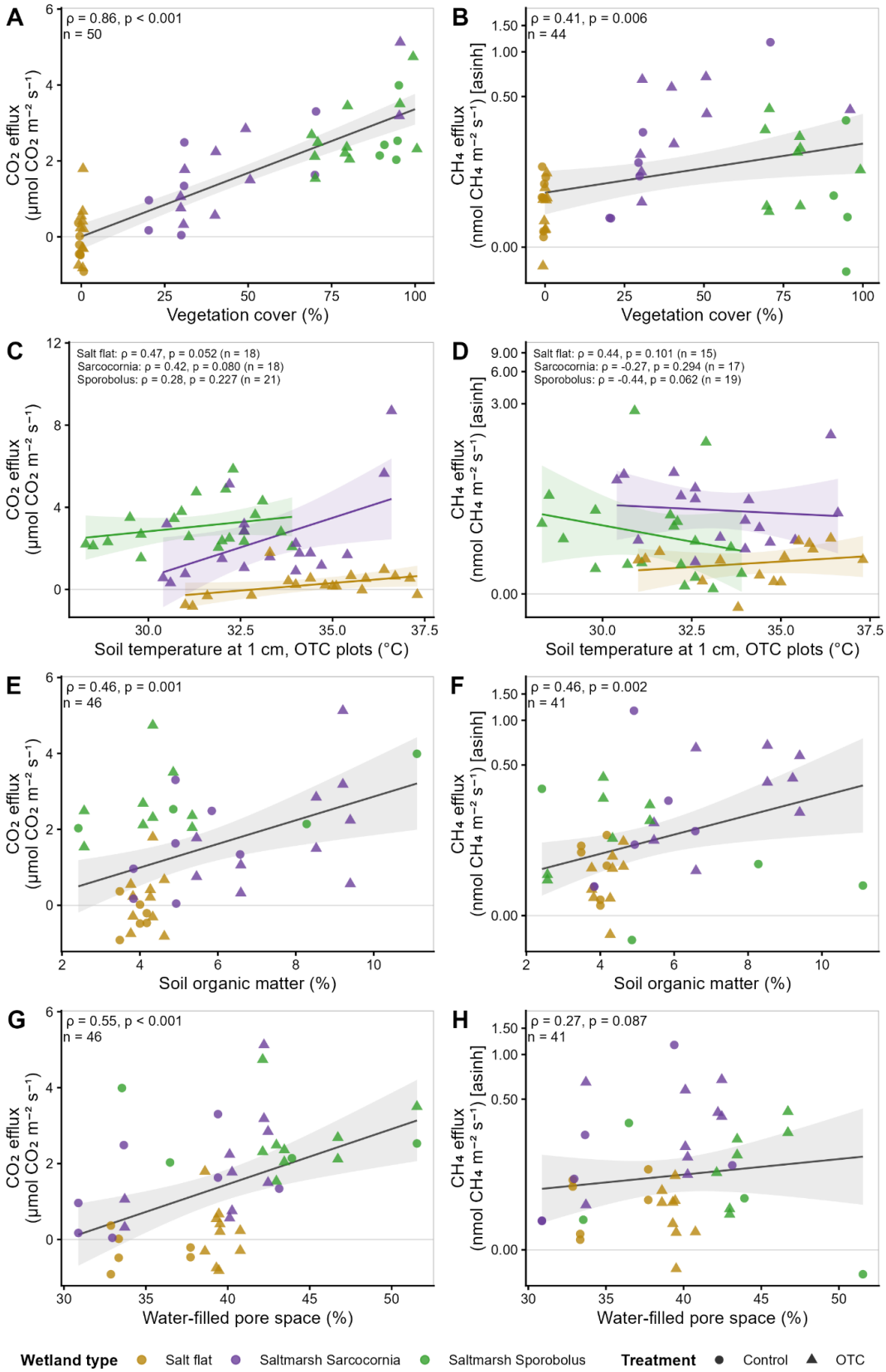


Figure 4. Relationships between CO_2 (left) and CH_4 (right, asinh scale) effluxes and (A, B) vegetation cover, (C, D) soil temperature at 1 cm (OTC plots only), (E, F) soil organic matter and (G, H) soil water-filled pore space (WFPS). Points are coloured by wetland type and shaped by treatment.

Study	Habitat	Condition	Location (lat.)	Climate; rain (mm)
Salt flat / hypersaline tidal flat				
This study	Salt flat	Dry season (Aug 2025)	Townsville (19.3°S)	Dry tropics; 1161
This study	Salt flat	Wet season, control	Townsville (19.3°S)	Dry tropics; 1161
This study	Salt flat	Wet season, OTC heatwave	Townsville (19.3°S)	Dry tropics; 1161
Brown et al. (2021)	Hypersaline flat	Annual sampling	Karumba (17.4°S)	Monsoon tropics; 883
Brown et al. (2021)	Hypersaline flat	Annual sampling	Gladstone (23.8°S)	Subtropics; 846
Lovelock et al. (2023)	Salt flat	BlueCAM emission factor	Australia	–
Saltmarsh				
This study	*S. quinqueflora*	Dry season (Aug 2025)	Townsville (19.3°S)	Dry tropics; 1161
This study	*S. quinqueflora*	Wet season, control	Townsville (19.3°S)	Dry tropics; 1161
This study	*S. quinqueflora*	Wet season, OTC heatwave	Townsville (19.3°S)	Dry tropics; 1161
This study	*S. virginicus*	Dry season (Aug 2025)	Townsville (19.3°S)	Dry tropics; 1161
This study	*S. virginicus*	Wet season, control	Townsville (19.3°S)	Dry tropics; 1161
This study	*S. virginicus*	Wet season, OTC heatwave	Townsville (19.3°S)	Dry tropics; 1161
Iram et al. (2021)	Saltmarsh	Seasonal means, 2018–20	Herbert River (18.9°S)	Wet tropics; 2158
Cadier et al. (2023)	Saltmarsh	Tidally connected	Burdekin (19.5°S)	Dry tropics; 656
Lovelock et al. (2023)	Saltmarsh	BlueCAM EF, monsoon/subtrop.	Australia	Monsoon/subtrop.
Lovelock et al. (2023)	Saltmarsh	BlueCAM EF, arid/temp./humid	Australia	Arid/temp./humid
Mangrove and freshwater wetlands				
Iram et al. (2021)	Mangrove	Seasonal means, 2018–20	Herbert River (18.9°S)	Wet tropics; 2158
Cadier et al. (2023)	Mangrove	Tidally connected	Burdekin (19.5°S)	Dry tropics; 656
Adame et al. (2026)	Mangrove	After extreme rainfall	Maroochy R. (26.6°S)	Subtropics
Lovelock et al. (2023)	Mangrove	BlueCAM EF, monsoon/subtrop.	Australia	Monsoon/subtrop.
Lovelock et al. (2023)	Mangrove	BlueCAM EF, arid/temp./humid	Australia	Arid/temp./humid
Iram et al. (2021)	Mangrove	Annual cumulative	Herbert River (18.9°S)	Wet tropics; 2158
Adame et al. (2026)	Restored wetland	After extreme rainfall	Maroochy R. (26.6°S)	Subtropics
Cadier et al. (2023)	Impounded (fresh)	Tidally restricted	Burdekin (19.5°S)	Dry tropics; 656

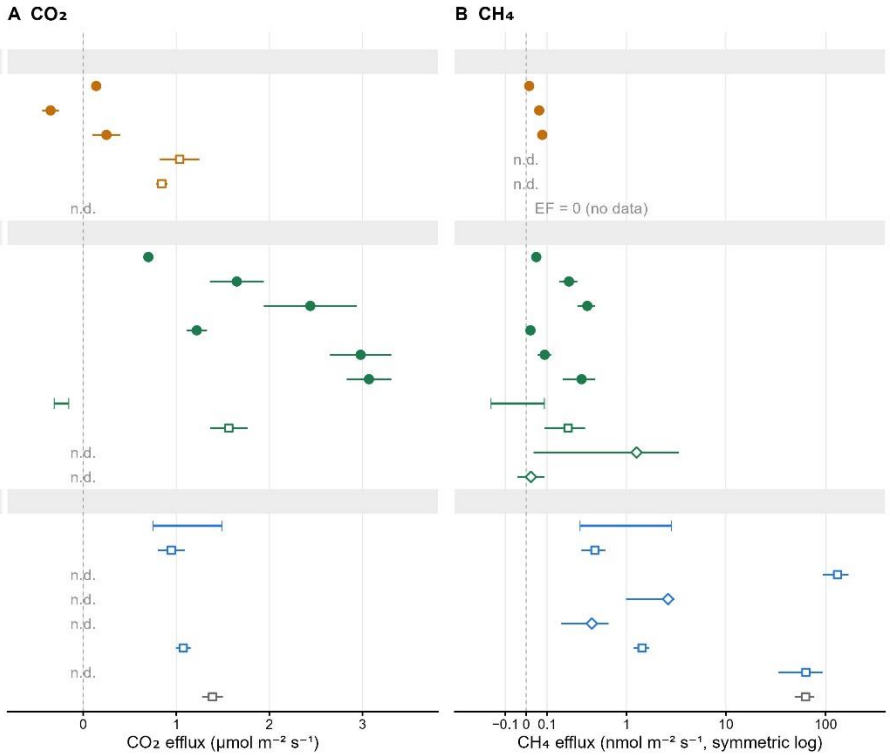


Figure 5. Comparison of CO_2 (A) and CH_4 (B) effluxes from this study with published values for hypersaline tidal flats, saltmarshes, mangroves and freshwater-impounded coastal wetlands in Australia. Values were converted to µmol CO_2 m^{-2} s^{-1} and nmol CH_4 m^{-2} s^{-1}. Filled circles show this study (mean ± SE). Open squares show literature means ± SE, bars with end ticks show ranges of seasonal means, and diamonds show BlueCAM emission factors (median and range; Lovelock et al. 2023). n.d. = no data. Most studies used dark chambers. CH_4 is shown on a symmetric log scale.

Discussion

Effect of vegetation presence in moderating CO_2 and CH_4 effluxes

Vegetation cover was the most important predictor of both CO_2 and CH_4 effluxes in the random forest models, followed by soil temperature and WFPS for CO_2. The effect of vegetation extended beyond the contrast between the unvegetated saltpan and the saltmarshes: efflux increased with cover across saltmarsh plots (Figure 4) and within *S. quinqueflora*, where cover ranged from 20 to 95%. Because the dark chambers enclosed the plants (above- and below-ground biomass) and sediments, the measured CO_2 effluxes included shoot and root respiration, suggesting that greater CO_2 effluxes in saltmarsh compared to saltpans were due to strong autotrophic respiration from live saltmarsh habitat (Morris & Whiting, 2024). For CH_4, vegetation can supply labile organic matter substrates to methanogens, and the greatest CH_4 effluxes are consistently observed in *S. quinqueflora* across all seasons and during heatwave simulation (Al-Haj & Fulweiler, 2020). In *S. virginicus*, despite denser canopy and a richer, well-connected shoot-root structure, CH_4 effluxes were lower than in *S. quinqueflora*, suggesting that CH_4 effluxes at this study site may be largely influenced by microbial processes rather than plant-mediated processes.

Simulated heatwave alters CO_2 and CH_4 effluxes in saltpans and saltmarshes

Our results provide experimental field evidence that responses of CO_2 and CH_4 effluxes to a simulated heatwave depend on wetland habitat types. Warming significantly increased CO_2 efflux in the unvegetated saltpan, switching it from CO_2 uptake to CO_2 emissions, an opposite observation to those in lower intertidal estuarine sandy sediments (Douglas et al., 2025). These contrasting findings may be due to differences in sediment properties across these studies, and particularly, we observed a significant saltpan surface cover by microbial mat during our sampling in the wet season (Table S1). In contrast to saltpans, CO_2 efflux in the *S. quinqueflora* and *S. virginicus* saltmarshes did not differ significantly between OTC and control plots, even though the OTCs warmed the soil surface by a similar amount in all three habitats (3.3–4.5 °C, Figure 2). This pattern is consistent with other findings that CO_2 effluxes in saltmarsh habitats are less sensitive to warming or temperature change, but temperature can play a key role in moderating their CO_2 exchange (Reef et al., 2025; Sun et al., 2022; Wei et al., 2026).

In *S. quinqueflora*, the slight increase in CO_2 efflux under the OTCs was consistent with temperature-driven stimulation of plant and soil respiration, and CO_2 efflux increased with soil temperature across days despite not being statistically different. In vegetation-dense *S. virginicus* plots, however, CO_2 efflux was unresponsive to warming, despite the largest warming (+4.5 °C, Figure 2D), and neither

CO_2 nor CH_4 was related to cover within these dense stands (70–100% cover). This suggests that respiration there was limited by factors other than temperature, such as substrate supply, oxygen availability in sediments with high water content, or a dominance of root respiration coupled to plant activity rather than to short-term warming (Figure 4). The dense *S. virginicus* canopy reduced warming of the soil surface in the OTCs (Figure 2C-D), which contrasted with the surface warming in the saltpan and *S. quinqueflora* where soil temperature at 1 cm remained elevated after OTC removal. This result indicated that high canopy cover in *S. virginicus* may limit heat transfer into the sediment, effectively insulating the soil. In the saltpan, which had no vascular plants, warming changed the direction and rate of CO_2 flux, suggesting altered sediment processes following the warming, for example, through reduced CO_2 uptake by the sediment microbial mats or enhanced respiration.

CH_4 efflux was low in all habitats, consistent with the constraints of sulfate reduction on methanogenesis in saline sediments (Arias-Ortiz et al., 2024; Kroeger et al., 2017; Poffenbarger et al., 2011). CH_4 efflux increased under warming in both vegetated saltmarsh habitats, which is consistent with previous studies on the temperature sensitivity of CH_4 efflux in coastal wetlands elsewhere (Burkholz et al., 2020; Lewis et al., 2026). This pattern suggests that warming acted via organic matter and microbial pathways, including enhanced methanogenesis and reduced CH_4 oxidation, in vegetated coastal wetlands. These differences in CO_2 and CH_4 efflux responses to the heating treatment among habitat types likely reflect structural differences among saltmarsh vegetation types and how these differences affect the soil surface.

Seasonal effects on CO_2 and CH_4 effluxes and comparison with other studies

Both CO_2 and CH_4 effluxes increased markedly from the dry to the wet season, by two to three times for CO_2 in the saltmarshes and three to five times for CH_4 in all habitats, highlighting strong seasonal control of greenhouse gas fluxes in these systems. *S. quinqueflora* also had the highest CH_4 efflux in both dry and wet seasons (Figure 2B), suggesting this habitat is consistently more favourable for methanogenesis. However, the measured environmental variables explained little variation in CH_4 efflux (cross-validated $R^2 = 0.03$, Figure 3), so its controls remain unresolved.

CO_2 and CH_4 efflux from these dry tropical saltpans and salt marshes were comparable with previous measurements across Australia and generally lower than other coastal wetland habitats, particularly mangroves (Figure 5). Mean CO_2 efflux ranged from net uptake in the saltpan (-0.35 µmol m^{-2} s^{-1}) to 3.1 µmol m^{-2} s^{-1} in *S. virginicus*, and mean CH_4 efflux ranged from 0.01 nmol m^{-2} s^{-1} in saltpans to 0.38 nmol m^{-2} s^{-1} in *S. quinqueflora* (Figure 2). These rates are within the range of those reported for coastal wetlands in Australia and globally (Al-Haj & Fulweiler, 2020; Rosentreter et al., 2023), and CH_4

efflux in particular was several orders of magnitude lower than in freshwater and tidal creeks in northern Australia (Adame et al., 2026; Cadier et al., 2023; Iram et al., 2021; Rosentreter et al., 2018; Sasmito et al., 2026).

Study limitations and future study implication

Several important caveats must be acknowledged for further interpretation of our study. First, our experiment simulated a single, low tide, seven-day heatwave event with occasional rain events during the simulation period and therefore the effects of repeated or prolonged heatwaves across successive seasons, which may progressively deplete labile soil carbon pools, alter plant physiology, or shift microbial community composition, remain unknown. Second, heatwaves in Australia occasionally co-occur with a pre-wet season dry period (November – January), conditions not replicated in our open-top chamber design. Third, while the unvegetated saltpan showed significant CO_2 stimulation, the absolute magnitude of this response, and its contribution to total ecosystem carbon budgets at the landscape scale, requires quantification against the much larger carbon fluxes of the vegetated zones. Finally, our study was conducted at a single site in the dry tropics of Northern Australia, and generalisability to other saltmarshes or other coastal wetland systems remains to be tested.

Future work could examine the effects of multiple consecutive heatwaves on GHG fluxes, explore the effect of heatwaves on ecosystem productivity (e.g., rates of gross primary productivity are reduced across terrestrial ecosystems at the continental scale (Bastos et al., 2014; Ciais et al., 2005)), explore whether saltmarsh resilience is maintained under compound drought-heat events, and investigate the tipping point of saltmarsh vegetation in modulating soil temperature anomalies and associated CO_2 and CH_4 fluxes during multiple scenarios of modified atmospheric heatwave events. Scaling our plot-level results to landscape-level GHG budgets using remote sensing of vegetation cover and saltpan extent will also be essential for incorporating heatwave vulnerability into blue carbon accounting frameworks in arid and monsoonal regions of Australia and globally.

In conclusion, CO_2 efflux in the unvegetated saltpan was sensitive to a simulated heatwave, whereas CO_2 efflux from vegetated saltmarshes was not different following sediment warming. Vegetation cover and types, soil temperature and moisture were among the major factors explaining CO_2 efflux in this study. CH_4 efflux, although low, increased under warming in vegetated saltmarshes. These contrasting responses indicate that vegetation shapes heatwave effects on coastal wetland greenhouse gas fluxes not only by modifying sediment temperature but through biological controls on respiration and methane production. Maintaining vegetated saltmarsh cover may therefore limit heatwave-driven CO_2 losses, although its effect on CH_4 efflux warrants further study. Overall, our

findings suggest that there are potential risks to the permanence of carbon storage and sinks in blue carbon ecosystems following intensifying heatwaves in a warming world. Therefore, future blue carbon methodology and emission factor refinement should take into account extreme events such as heatwaves.

Acknowledgement

We thank the First Nation people for the land on which this research was completed and pay respect to their elders, past, present and emerging. We thank Antony Squires, who assisted with GHG sampling collar and OTC preparation. We thank Townsville City Council, which provided access to the field site at Oonoonba Wetlands as part of the Townsville Living Coastline Project. This study was supported by James Cook University Research Grant Scheme to SDS and RM. Open access to this paper was supported by James Cook University as a member of the Council of Australian University Librarians (CAUL) consortium.

References

Adame, M. F., Iram, N., Hall, J. M., Grundy, N. J., Pearse, A., Bennion, V., Lovelock, C. E., Rummell, A. J., Marshall, S., Webb, G., Glamore, W., Chalmers, G., Olds, A. D., Keith, H., & Smart, J. C. R. (2026). Restored and reference coastal wetlands emit elevated levels of methane after an extreme rainfall event, but continue to provide climate benefits. *Environmental Research Letters*, *21*(13), 134029. https://doi.org/10.1088/1748-9326/ae7e0b

Adame, M. F., Kelleway, J., Krauss, K. W., Lovelock, C. E., Adams, J. B., Trevathan-Tackett, S. M., Noe, G., Jeffrey, L., Ronan, M., Zann, M., Carnell, P. E., Iram, N., Maher, D. T., Murdiyarso, D., Sasmito, S., Tran, D. B., Dargusch, P., Kauffman, J. B., & Brophy, L. (2024). All tidal wetlands are blue carbon ecosystems. *BioScience*, *74*(4), 253–268. https://doi.org/10.1093/biosci/biae007

Adame, M. F., Reef, R., Grinham, A., Holmes, G., & Lovelock, C. E. (2012). Nutrient exchange of extensive cyanobacterial mats in an arid subtropical wetland. *Marine & Freshwater Research*, *63*(5), 457–467. https://doi.org/10.1071/MF11133

Al-Haj, A. N., & Fulweiler, R. W. (2020). A synthesis of methane emissions from shallow vegetated coastal ecosystems. *Global Change Biology*, *26*(5), 2988–3005. https://doi.org/10.1111/gcb.15046

An, Z., Bork, E. W., Olefeldt, D., Carlyle, C. N., & Chang, S. X. (2022). Simulated heat wave events increase CO2 and N2O emissions from cropland and forest soils in an incubation experiment. *Biology and Fertility of Soils*, *58*(7), 789–802. https://doi.org/10.1007/s00374-022-01661-w

Arias-Ortiz, A., Serrano, O., Masqué, P., Lavery, P. S., Mueller, U., Kendrick, G. A., Rozaimi, M., Esteban, A., Fourqurean, J. W., Marbà, N., Mateo, M. A., Murray, K., Rule, M. J., & Duarte, C. M. (2018). A marine heatwave drives massive losses from the world's largest seagrass

carbon stocks. *Nature Climate Change*, *8*(4), 338–344. https://doi.org/10.1038/s41558-018-0096-y

Arias-Ortiz, A., Wolfe, J., Bridgham, S. D., Knox, S., McNicol, G., Needelman, B. A., Shahan, J., Stuart-Haëntjens, E. J., Windham-Myers, L., Oikawa, P. Y., Baldocchi, D. D., Caplan, J. S., Capooci, M., Czapla, K. M., Derby, R. K., Diefenderfer, H. L., Forbrich, I., Groseclose, G., Keller, J. K., … Holmquist, J. R. (2024). Methane fluxes in tidal marshes of the conterminous United States. *Global Change Biology*, *30*(9), e17462. https://doi.org/10.1111/gcb.17462

Bastos, A., Gouveia, C. M., Trigo, R. M., & Running, S. W. (2014). Analysing the spatio-temporal impacts of the 2003 and 2010 extreme heatwaves on plant productivity in Europe. *Biogeosciences*, *11*(13), 3421–3435. https://doi.org/10.5194/bg-11-3421-2014

Burkholz, C., Garcias-Bonet, N., & Duarte, C. M. (2020). Warming enhances carbon dioxide and methane fluxes from Red Sea seagrass (*Halophila stipulacea*) sediments. *Biogeosciences*, *17*(7), 1717–1730. https://doi.org/10.5194/bg-17-1717-2020

Cadier, C., Waltham, N. J., Canning, A., Fry, S., & Adame, M. F. (2023). Tidal restoration to reduce greenhouse gas emissions from freshwater impounded coastal wetlands. *Restoration Ecology*, *31*(8), e13829. https://doi.org/10.1111/rec.13829

Carey, J. C., Kroeger, K. D., & Tang, J. (2022). Higher Temperature Sensitivity of Ecosystem Respiration in Low Marsh Compared to High Elevation Marsh Ecosystems. *Journal of Geophysical Research: Biogeosciences*, *127*(11), e2022JG006832. https://doi.org/10.1029/2022JG006832

Chung, C. T. Y., Hope, P., Hutley, L. B., Brown, J., & Duke, N. C. (2023). Future climate change will increase risk to mangrove health in Northern Australia. *Communications Earth & Environment*, *4*(1), 192. https://doi.org/10.1038/s43247-023-00852-z

Ciais, P., Reichstein, M., Viovy, N., Granier, A., Ogée, J., Allard, V., Aubinet, M., Buchmann, N., Bernhofer, C., Carrara, A., Chevallier, F., De Noblet, N., Friend, A. D., Friedlingstein, P.,

Grünwald, T., Heinesch, B., Keronen, P., Knohl, A., Krinner, G., … Valentini, R. (2005). Europe-wide reduction in primary productivity caused by the heat and drought in 2003. *Nature*, *437*(7058), 529–533. https://doi.org/10.1038/nature03972

DETSI. (2019). *Intertidal mud above mean sea level unconsolidated mud (claypan/saltpan)*. Queensland Government. WetlandInfo Website. https://wetlandinfo.detsi.qld.gov.au/wetlands/ecology/aquatic-ecosystems-natural/estuarine-marine/descriptions/27/

Douglas, E. J., Lam-Gordillo, O., Hailes, S. F., Lohrer, A. M., & Cummings, V. J. (2025). Simulated heatwave alters intertidal estuary greenhouse gas fluxes. *Nature Communications*, *16*(1), 10507. https://doi.org/10.1038/s41467-025-65519-z

Filbee-Dexter, K., Gendall, L., Pessarrodona, A., Burrows, M. T., Gupta, A. S., Hobday, A. J., Holbrook, N. J., Malan, N., Montie, S., Krumhansl, K. A., Moore, P. J., Oliver, E. C. J., Smale, D. A., Smith, K. E., Starko, S. A., Thomsen, M., Vanderklift, M., Zhao, Z., & Wernberg, T. (2026). *Marine heatwaves drive widespread loss and slow recovery of coastal carbon cycling*. In Review. https://doi.org/10.21203/rs.3.rs-9834051/v1

Hickey, S. M., Stone, A., Radford, B., & Lovelock, C. E. (2025). Multidecadal mapping of arid intertidal ecosystems reveals a dynamic mosaic of habitats north-western Australia. *Estuarine, Coastal and Shelf Science*, *323*, 109401. https://doi.org/10.1016/j.ecss.2025.109401

Iram, N., Kavehei, E., Maher, D. T., Bunn, S. E., Rezaei Rashti, M., Farahani, B. S., & Adame, M. F. (2021). Soil greenhouse gas fluxes from tropical coastal wetlands and alternative agricultural land uses. *Biogeosciences*, *18*(18), 5085–5096. https://doi.org/10.5194/bg-18-5085-2021

Kroeger, K. D., Crooks, S., Moseman-Valtierra, S., & Tang, J. (2017). Restoring tides to reduce methane emissions in impounded wetlands: A new and potent Blue Carbon climate

change intervention. *Scientific Reports*, *7*(1), 11914. https://doi.org/10.1038/s41598-017-12138-4

Leggat, W. P., Camp, E. F., Suggett, D. J., Heron, S. F., Fordyce, A. J., Gardner, S., Deakin, L., Turner, M., Beeching, L. J., Kuzhiumparambil, U., Eakin, C. M., & Ainsworth, T. D. (2019). Rapid Coral Decay Is Associated with Marine Heatwave Mortality Events on Reefs. *Current Biology*, *29*(16), 2723-2730.e4. https://doi.org/10.1016/j.cub.2019.06.077

Lei, X., Shen, Y., Zhao, J., Huang, J., Wang, H., Yu, Y., & Xiao, C. (2023). Root Exudates Mediate the Processes of Soil Organic Carbon Input and Efflux. *Plants*, *12*(3), 630. https://doi.org/10.3390/plants12030630

Lewis, A. S. L., Rich, R. L., & Noyce, G. L. (2026). Warming Amplifies the Variability of Methane Emissions From a Coastal Wetland. *Journal of Geophysical Research: Biogeosciences*, *131*(10), e2026JG009973. https://doi.org/10.1029/2026JG009973

Lovelock, C. E., & Duarte, C. M. (2019). Dimensions of Blue Carbon and emerging perspectives. *Biology Letters*, *15*(3), 20180781. https://doi.org/10.1098/rsbl.2018.0781

Lovelock, C. E., Grinham, A., Adame, M. F., & Penrose, H. M. (2010). Elemental composition and productivity of cyanobacterial mats in an arid zone estuary in north Western Australia. *Wetlands Ecology and Management*, *18*(1), 37–47. https://doi.org/10.1007/s11273-009-9146-6

Määttä, T., & Malhotra, A. (2024). The hidden roots of wetland methane emissions. *Global Change Biology*, *30*(2), e17127. https://doi.org/10.1111/gcb.17127

Macreadie, P. I., Costa, M. D. P., Atwood, T. B., Friess, D. A., Kelleway, J. J., Kennedy, H., Lovelock, C. E., Serrano, O., & Duarte, C. M. (2021). Blue carbon as a natural climate solution. *Nature Reviews Earth & Environment*, *2*(12), 826–839. https://doi.org/10.1038/s43017-021-00224-1

Malerba, M. E., Friess, D. A., Peacock, M., Grinham, A., Taillardat, P., Rosentreter, J. A., Webb, J., Iram, N., Al-Haj, A. N., & Macreadie, P. I. (2022). Methane and nitrous oxide emissions

complicate the climate benefits of teal and blue carbon wetlands. *One Earth*, *5*(12), 1336–1341. https://doi.org/10.1016/j.oneear.2022.11.003

Morris, J. T., & Whiting, G. J. (2024). Components of the CO2 Exchange in a Southeastern USA Salt Marsh. *Ocean-Land-Atmosphere Research*, *3*, 0077. https://doi.org/10.34133/olar.0077

Perkins-Kirkpatrick, S. E., & Lewis, S. C. (2020). Increasing trends in regional heatwaves. *Nature Communications*, *11*(1), 3357. https://doi.org/10.1038/s41467-020-16970-7

Poffenbarger, H. J., Needelman, B. A., & Megonigal, J. P. (2011). Salinity Influence on Methane Emissions from Tidal Marshes. *Wetlands*, *31*(5), 831–842. https://doi.org/10.1007/s13157-011-0197-0

Queensland Government. (2019). *Field guide to common saltmarsh plants of Queensland* [Text]. The State of Queensland. https://www.publications.qld.gov.au/dataset/common-saltmarsh-plants-of-queensland/resource/a5962a08-c3af-4aba-80b5-dfd232b5cef3

Reef, R., Daly, E., Anandappa, T., Vienna-Hallam, E.-J., Robertson, H., Peck, M., & Guyot, A. (2025). Eddy covariance evaluation of ecosystem fluxes at a temperate saltmarsh in Victoria, Australia, shows large CO_2 uptake. *Biogeosciences*, *22*(4), 1149–1162. https://doi.org/10.5194/bg-22-1149-2025

Rosentreter, J. A., Al-Haj, A. N., Fulweiler, R. W., & Williamson, P. (2021). Methane and Nitrous Oxide Emissions Complicate Coastal Blue Carbon Assessments. *Global Biogeochemical Cycles*, *35*(2). https://doi.org/10.1029/2020GB006858

Rosentreter, J. A., Laruelle, G. G., Bange, H. W., Bianchi, T. S., Busecke, J. J., Cai, W.-J., Eyre, B. D., Forbrich, I., Kwon, E. Y., & Maavara, T. (2023). Coastal vegetation and estuaries are collectively a greenhouse gas sink. *Nature Climate Change*, 1–9.

Rosentreter, J. A., Maher, D. T., Erler, D. V., Murray, R., & Eyre, B. D. (2018). Factors controlling seasonal CO2 and CH4 emissions in three tropical mangrove-dominated estuaries in

Australia. *Estuarine, Coastal and Shelf Science*, *215*, 69–82. https://doi.org/10.1016/j.ecss.2018.10.003

Sang, W., Yang, H., Feng, W., Chen, H., Tang, J., & Chen, S. (2026). Unlocking the Impact of Temperature and Salinity on Greenhouse Gas Emissions From Estuarine Salt Marsh Soils. *Earth's Future*, *14*(2), e2025EF006912. https://doi.org/10.1029/2025EF006912

Sasmito, S. D., Mishra, A. K., Duvert, C., Montagna, L., Barkley, A. S., Widanto, D. S., Mulloy, R., Cartwright, P., & Waltham, N. J. (2026). Contrasting sediment and aquatic CO2 and CH4 effluxes across Australian tropical salt flat, saltmarsh, mangrove and tidally restricted wetlands. *Estuarine, Coastal and Shelf Science*, *330*, 109693. https://doi.org/10.1016/j.ecss.2025.109693

Smith, K. E., Aubin, M., Burrows, M. T., Filbee-Dexter, K., Hobday, A. J., Holbrook, N. J., King, N. G., Moore, P. J., Sen Gupta, A., Thomsen, M., Wernberg, T., Wilson, E., & Smale, D. A. (2024). Global impacts of marine heatwaves on coastal foundation species. *Nature Communications*, *15*(1), 5052. https://doi.org/10.1038/s41467-024-49307-9

Sun, B., Jiang, M., Han, G., Zhang, L., Zhou, J., Bian, C., Du, Y., Yan, L., & Xia, J. (2022). Experimental warming reduces ecosystem resistance and resilience to severe flooding in a wetland. *Science Advances*, *8*(4), eabl9526. https://doi.org/10.1126/sciadv.abl9526

Wei, S., Chu, X., Sun, B., Sun, R., Zhang, X., Song, W., Wang, X., Pendall, E., & Han, G. (2026). Climate Warming Impaired the CO2 Sink Capacity and Efficiency in a Suaeda salsa-Dominated Salt Marsh. *Global Change Biology*, *32*(10), e71151. https://doi.org/10.1111/gcb.71151

Whitcraft, C. R., & Levin, L. A. (2007). Regulation of Benthic Algal and Animal Communities by Salt Marsh Plants: Impact of Shading. *Ecology*, *88*(4), 904–917. https://doi.org/10.1890/05-2074

Worthington, T. A., Spalding, M., Landis, E., Maxwell, T. L., Navarro, A., Smart, L. S., & Murray, N. J. (2024). The distribution of global tidal marshes from Earth observation data. *Global Ecology and Biogeography*, *33*(8), e13852. https://doi.org/10.1111/geb.13852

Xu, W., Wu, D., Ciais, P., Wang, Y.-P., Huang, M., Yuan, W., & Liu, J. (2026). Earlier and faster heatwave onset on land under a warming climate. *Nature Climate Change*. https://doi.org/10.1038/s41558-026-02762-2

Supplementary Information

Table S1. Monthly rainfall and daily maximum air temperature at Townsville from January 2025 to September 2026, covering the dry-season (August 2025) and wet-season heatwave (March 2026) sampling campaigns.

		Rainfall (mm)					Daily maximum air temperature (°C)				
Year	Month	Total	Rain days (≥1 mm)	Highest daily	Long-term mean	% of long-term mean	Mean	Lowest	Highest	Long-term mean	Anomaly
2025	Jan	148.2	11	51.2	274.4	54	32.9	26.3	37.0	31.5	+1.4
	Feb	1198.0	17	284.0	312.9	383	30.8	25.2	37.7	31.2	-0.4
	Mar	1004.6	20	301.4	197.9	508	30.7	26.7	34.0	30.8	-0.1
	Apr	107.8	7	33.0	66.7	162	30.1	27.4	32.3	29.7	+0.4
	May	49.2	3	33.8	33.7	146	29.1	23.4	31.3	27.7	+1.4
	Jun	24.8	4	11.0	20.1	123	26.4	20.3	31.5	25.7	+0.7
	Jul	16.4	5	5.2	15.5	106	26.4	23.8	28.9	25.2	+1.2
	Aug*	**0.0**	**0**	**0.0**	**15.7**	**0**	**27.2**	**20.7**	**32.0**	**26.2**	**+1.0**
	Sep	0.8	0	0.4	9.9	8	29.1	26.5	32.3	27.9	+1.2
	Oct	5.2	3	2.0	23.2	22	31.9	29.9	36.4	29.6	+2.3
	Nov	60.4	6	24.2	60.7	100	33.2	30.8	36.1	30.9	+2.3
	Dec	335.4	10	142.2	130.3	257	32.1	25.8	36.3	31.6	+0.5
2026	Jan	657.2	16	223.0	274.4	240	30.6	25.8	34.8	31.5	-0.9
	Feb	353.8	13	73.8	312.9	113	31.3	27.9	33.7	31.2	+0.1
	Mar*	**145.0**	**15**	**27.2**	**197.9**	**73**	**30.9**	**28.6**	**32.2**	**30.8**	**+0.1**
	Apr	14.8	4	5.4	66.7	22	30.6	26.3	32.4	29.7	+0.9
	May	0.0	0	0.0	33.7	0	28.9	25.9	31.0	27.7	+1.2
	Jun	4.0	1	3.0	20.1	20	27.5	24.6	28.7	25.7	+1.8
	Jul	0.0	0	0.0	15.5	0	26.7	25.2	28.7	25.2	+1.5
	Aug	0.0	0	0.0	15.7	0	27.2	24.9	31.0	26.2	+1.0
	Sep	9.2	1	8.4	9.9	93	28.1	25.8	29.8	27.9	+0.2

* Sampling months (shaded): dry season, 7 and 19 August 2025; wet-season simulated heatwave, 10–16 March 2026.

Data: Bureau of Meteorology Climate Data Online, station 032040 Townsville Aero (19.25°S, 146.77°E), daily rainfall (IDCJAC0009) and daily maximum temperature (IDCJAC0010). Daily rainfall is the 24 h total to 09:00. Long-term means are for all years of record at the station (from 1940).

Anomaly = monthly mean daily maximum temperature minus the long-term mean for that month. October 2025 has one missing temperature day (n = 30).

577 Table S2. Summary of field conditions of the established OTC and control plots

Plot ID	Habitat	Plot types (OTC vs Control)	Vegetation types and cover	Number of crab burrows	Photo of the plot
01	Tidal Flat	Control	Algae 100%	0	
02	Tidal Flat	OTC	Algae 100%	0	
03	Tidal Flat	OTC	Algae 100%	0	
04	Tidal Flat	OTC	Algae 100%	0	
05	Tidal Flat	Control	Algae 100%	0	
06	Tidal Flat	Control	Algae 100%	0	
07	Tidal Flat	OTC	Algae 100%	0	

08	Tidal Flat	Control	Algae 100%	0	
09	Tidal Flat	OTC	Algae 100%	0	
10	Tidal Flat	Control	Algae 100%	0	
11	Sarcocornia	OTC	Sarcocornia 30%	9	
12	Sarcornia	Control	Sarcocornia 30%	1	
13	Sarcornia	OTC	Sarcocornia 30%	7	
14	Sarcornia	Control	Sarcocornia 20%	0	
15	Sarcornia	OTC	Sarcocornia 95%	3	

16	Sarcornia	Control	Sarcocornia 70%	4	
17	Sporobolus	OTC	Sporobolus 70%	4	
18	Sporobolus	Control	Sporobolus 95%	2	
19	Sporobolus	OTC	Sporobolus 100%	0	
20	Sporobolus	Control	Sporobolus 95%	3	
21	Sarcocornia	OTC	Sarcocornia 40%	4	
22	Sarcocornia	Control	Sarcocornia 30%	9	
23	Sarcocornia	OTC	Sarcocornia 50%	5	

24	Sarcocornia	Control	Sarcocornia 30%	6	
25					
26	Sporobolus	Control	Sporobolus 90%	11	
27	Sporobolus	OTC	Sporobolus 80%	6	
28	Sporobolus	Control	Sporobolus 95%	21	
29	Sporobolus	OTC	Sporobolus 80%	21	
30	Sporobolus	OTC	Sporobolus 70%	10	
31	Sporobolus	OTC	Sporobolus 95%	8	
32	Sporobolus	Control	Sporobolus 90%	9	

578

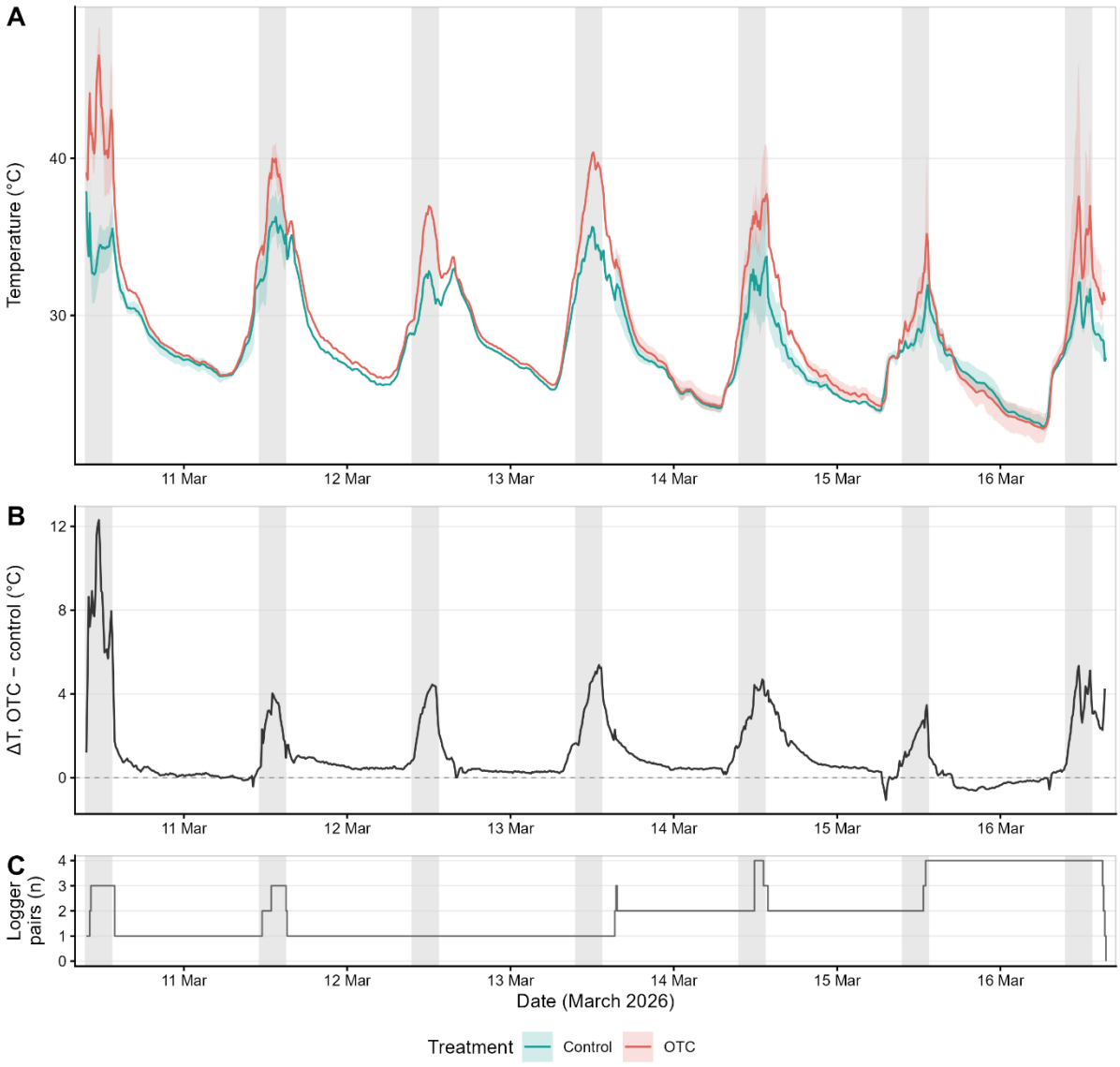
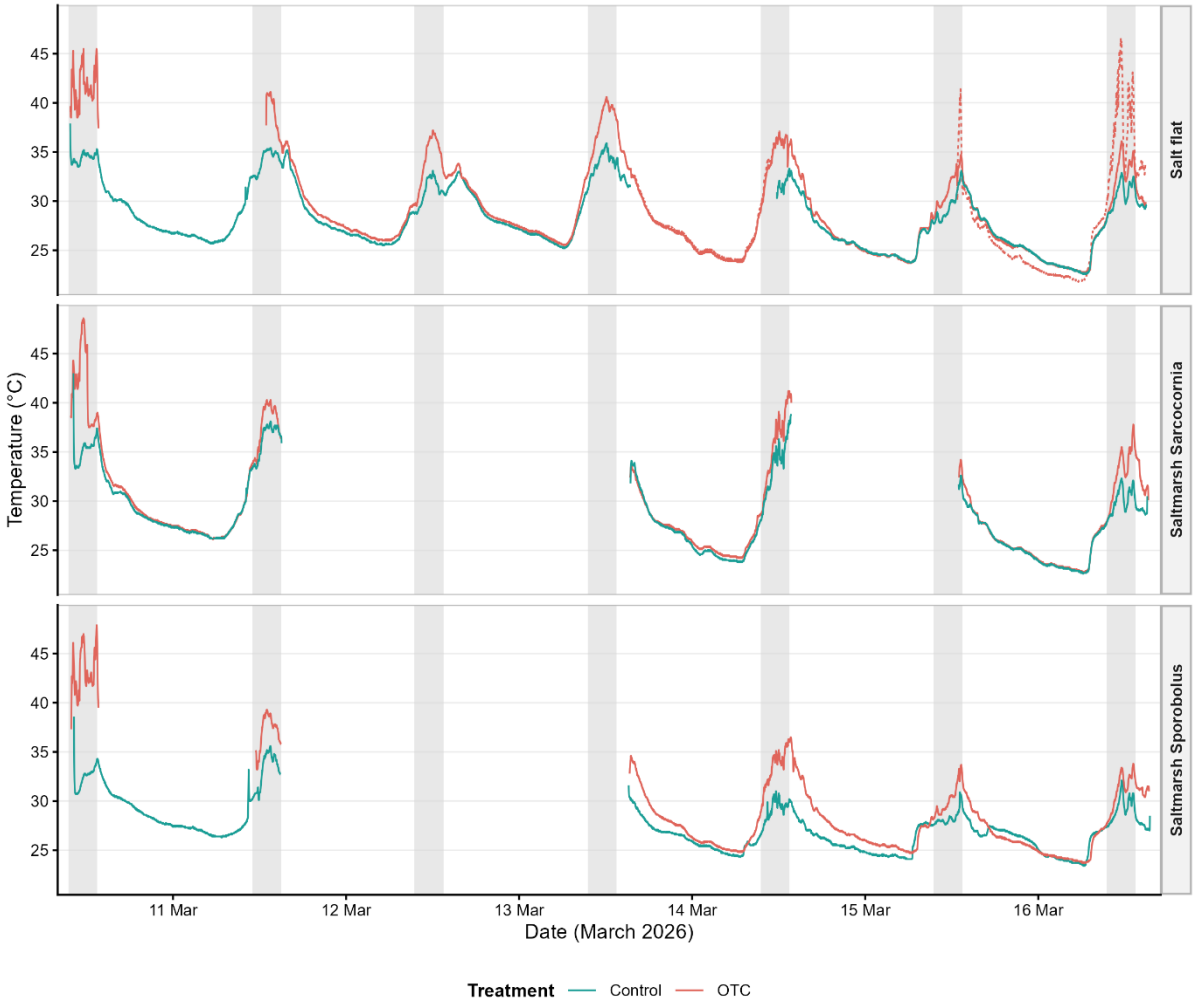


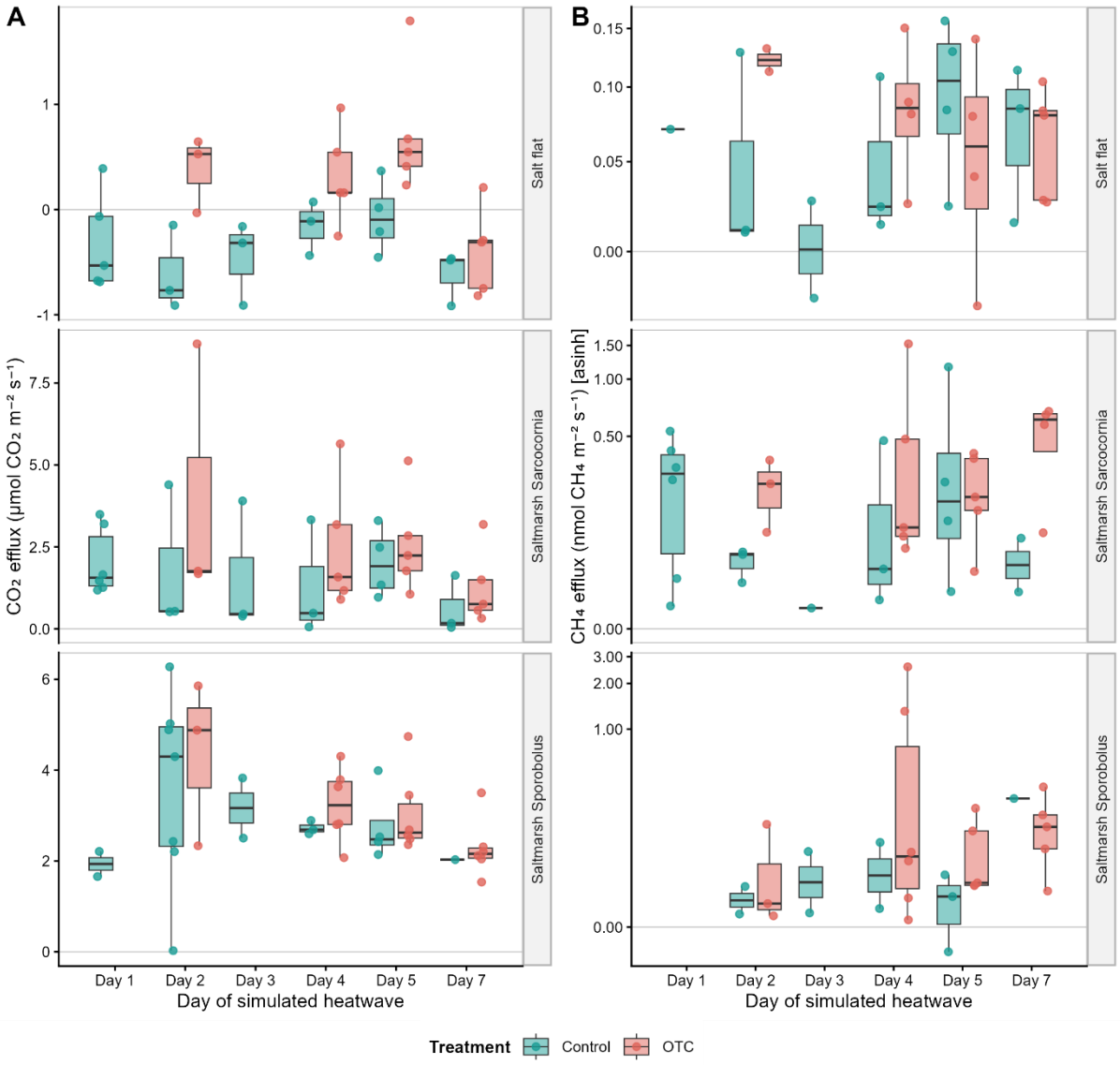
Figure S1. Temperature during the simulated heatwave combined across wetland types. (A) Mean temperature of OTC and control loggers (lines), with the range across loggers (bands). **(B)** Mean warming (OTC minus paired control). **(C)** Number of logger pairs recording at each time. From 11 to 13 March, only the salt-flat pair was recording due to limited availability of the temperature loggers. Grey bands mark daily simulated heatwave windows.



585

586 **Figure S2. Continuous temperature recorded by loggers in OTC (red) and control (teal) plots in each**
587 **wetland type during the simulated heatwave sampling period, 10–16 March 2026.** Grey bands
588 mark daily heatwave windows when OTCs were installed (09:30–13:30; 11:00–15:00 on 11 March
589 2026). The dashed line shows the second salt-flat OTC logger, deployed from 13 March. Gaps indicate
590 periods without logger data.

591



592

593 **Figure S3. Daily CO_2 and CH_4 fluxes during simulated heatwave.** Daily CO_2 **(A)** and CH_4 **(B)** efflux in
594 control and OTC plots in each wetland type during the simulated heatwave, 10–16 March 2026.
595 Boxes show the median and interquartile range, and points are individual measurements. OTC plots
596 were not measured on Days 1 and 3 due to logistical issues in the field.

597

598

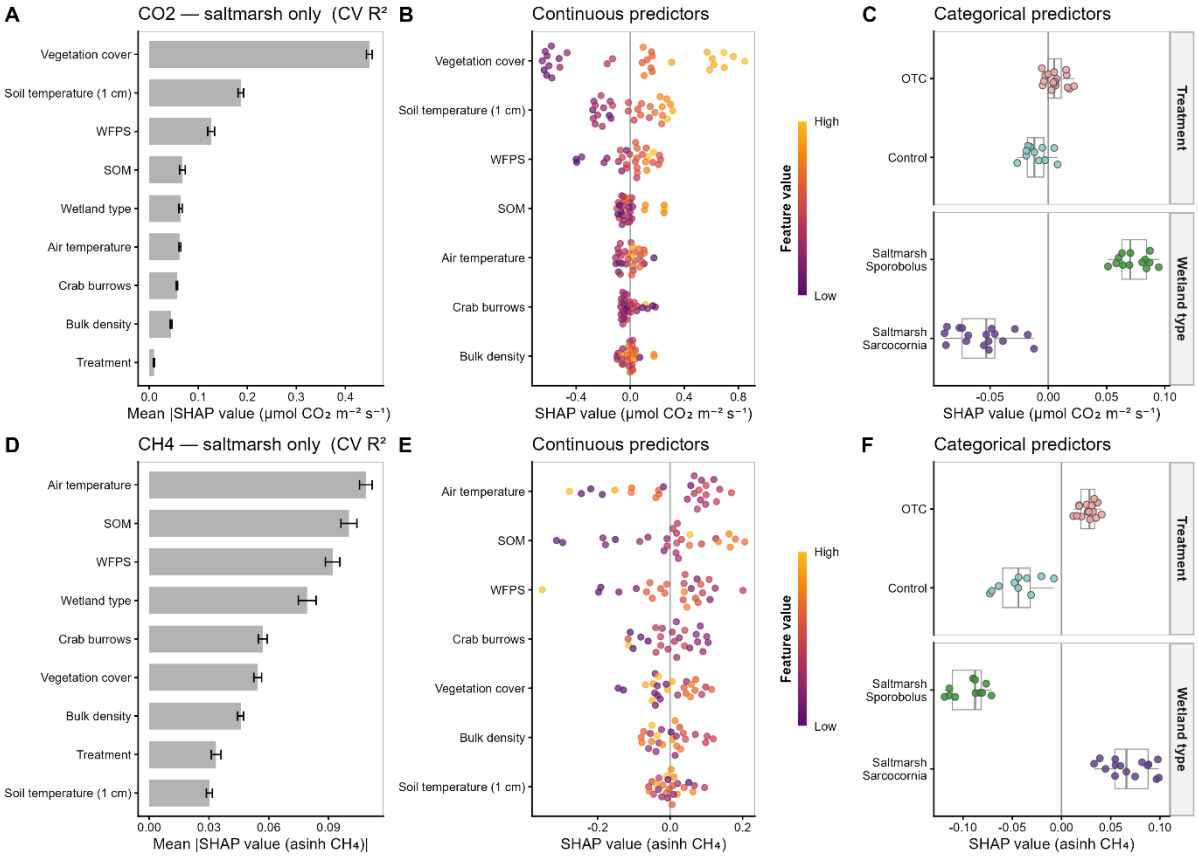
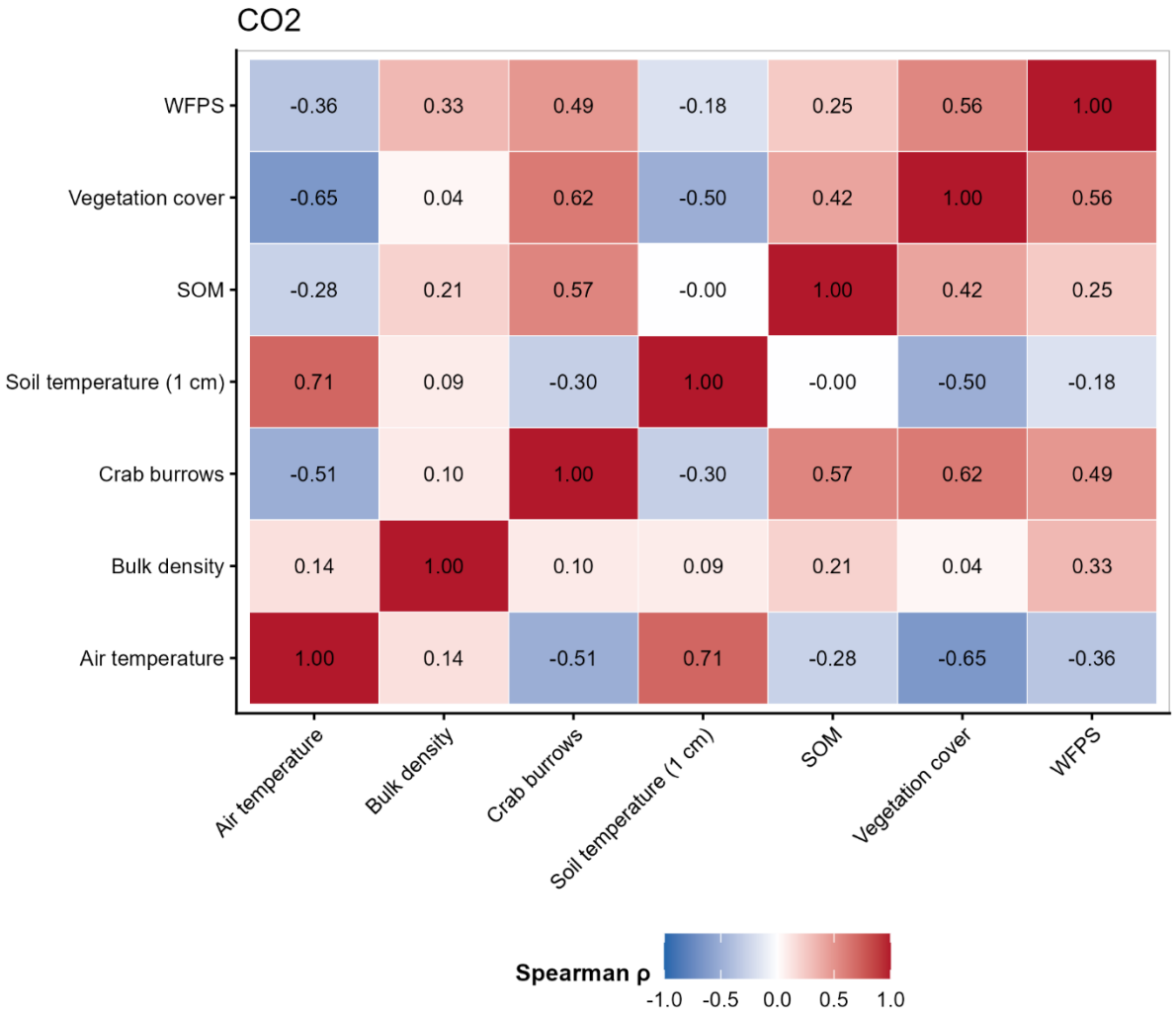


Figure S4. Saltmarsh SHAP analysis results. Predictor importance for CO_2 **(A)** and CH_4 **(B)** efflux, from models fitted to saltmarsh plots only data, with the salt flat excluded.



602

603 **Figure S5. Predictor correlations for CO2 flux.** Spearman correlations among the continuous
604 predictors used in the random forest models. Pairs with ρ > 0.7 were checked for redundancy; soil
605 and air temperature (ρ = 0.71) share importance.

606

607